

Preparation and Structure of $\text{Re}(\equiv\text{NC}_6\text{H}_5)(\text{PPh}_3)(\text{PR}_3)\text{Cl}_3$, $\text{PR}_3 = \text{PMe}_3, \text{P}(\text{OMe})_3$

Young-woong Kim, June-ho Jung, Hee-sook Park, and Soon W. Lee*

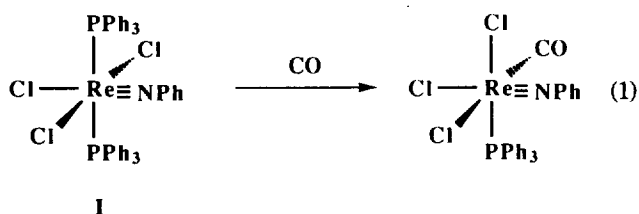
Department of Chemistry, Sung Kyun Kwan University, Suwon 440-746, Korea

Received July 16, 1994

Reactions of *mer, trans*- $\text{Re}(\equiv\text{NC}_6\text{H}_5)(\text{PPh}_3)_2\text{Cl}_3$, **I**, with PMe_3 and $\text{P}(\text{OMe})_3$ at room temperature, led to *mer, trans*- $\text{Re}(\equiv\text{NC}_6\text{H}_5)(\text{PPh}_3)(\text{PMe}_3)\text{Cl}_3$, **II**, and *fac*- $\text{Re}(\equiv\text{NC}_6\text{H}_5)(\text{PPh}_3)(\text{P}(\text{OMe})_3)\text{Cl}_3$, **III**, respectively. The crystal structures of **II** and **III** were determined through X-ray diffraction. **II** crystallizes in the orthorhombic system, space group $Pna2_1$ with cell parameters $a = 19.379(4)$ Å, $b = 11.867(2)$ Å, $c = 12.676(3)$ Å, and $Z = 4$. Least-squares refinement of the structure led to a $R(wR_2)$ factor of 0.0251 (0.0621) for 2203 unique reflections of $I > 2\sigma(I)$ and for 306 variables. **III** crystallizes in the monoclinic system, space group $P2_1/n$ with cell parameters $a = 11.399(3)$ Å, $b = 14.718(4)$ Å, $c = 17.558(5)$ Å, $\beta = 97.79(2)^\circ$, and $Z = 4$. Least-squares refinement of the structure led to a $R(wR_2)$ factor of 0.0571 (0.1384) for 3739 unique reflections of $I > 2\sigma(I)$ and for 344 variables. Structural studies showed that the relative orientations of the two phosphines in both complexes are different, probably due to the differences in the coordinating abilities between PMe_3 and $\text{P}(\text{OMe})_3$ to the 5-coordinate fluxional intermediate.

Introduction

Since 1959 transition-metal imido (or nitrene) complexes have been reported, including derivatives of Group 4-8 metals, and have attracted continuous interest.¹ They have been postulated to be important intermediates in a several industrial catalytic processes.²⁻⁴ Bergman and his workers recently reported an insertion of CO into an $\text{Ir} \equiv \text{N}$ bond in $\text{Cp}^*\text{Ir}(\equiv\text{N}^t\text{Bu})(\text{Cp}^* = \text{C}_5(\text{CH}_3)_5)$, which is the first carbonylation of a terminal imido ligand to give an isocyanate complex.⁵ Very recently, our group reported the preparation and structure of *fac*- $\text{Re}(\equiv\text{NPh})(\text{CO})(\text{PPh}_3)\text{Cl}_3$, by treating *mer, trans*- $\text{Re}(\equiv\text{NPh})(\text{PPh}_3)_2\text{Cl}_3$, **I**, with CO Eq. (1).⁶ Our initial purpose in that experiment is to induce an insertion of CO into a $\text{Re} \equiv \text{N}$ bond to transform a terminal nitrene into an isocyanate group. The results of studies, however, revealed that the product results from substitution instead of insertion. We decided to modify the ligand environments of **I** by replacing PPh_3 with the smaller ligands, PMe_3 and $\text{P}(\text{OMe})_3$, possessing the better coordinating ability. We report here the preparations and structures of *mer, trans*- $\text{Re}(\equiv\text{NC}_6\text{H}_5)(\text{PPh}_3)(\text{PMe}_3)\text{Cl}_3$, **II**, and *fac*- $\text{Re}(\equiv\text{NC}_6\text{H}_5)(\text{PPh}_3)(\text{PMe}_3)\text{Cl}_3$, **II**, and *fac*- $\text{Re}(\equiv\text{NC}_6\text{H}_5)(\text{PPh}_3)(\text{P}(\text{OMe})_3)\text{Cl}_3$, **III**.



Experimental

Unless otherwise stated, all the reactions have been performed with standard Schlenk line and cannula techniques under an argon atmosphere. Air-sensitive solids were manipulated in a glove box filled with an argon gas. Glassware was either flame-dried or oven-dried. Benzene, diethyl ether,

tetrahydrofuran (THF), and hydrocarbon solvents were stirred over sodium metal and distilled under vacuum. NMR solvents (C_6D_6 and CDCl_3) were freeze-pump-thaw degassed before use and stored over molecular sieves under argon. Aniline was distilled from CaH_2 and stored under argon. Re , trimethylphosphine (PMe_3 ; $\text{Me} = \text{CH}_3$, 1 M in toluene), trimethylphosphite ($\text{P}(\text{OMe})_3$), and triphenylphosphine (PPh_3 ; $\text{Ph} = \text{C}_6\text{H}_5$) were purchased from Aldrich Co. and used as received. $\text{Re}(\equiv\text{NC}_6\text{H}_5)(\text{PPh}_3)\text{Cl}_3$, **I**, was prepared by the literature method.⁷

¹H and ¹³C NMR spectra were recorded with a Hitach 1100 60-MHz spectrometer and a Varian 200-MHz spectrometer with reference to tetramethylsilane. IR spectra were recorded with a Nicolet 205 FTIR spectrophotometer. Melting points were measured with a Thomas Hoover capillary melting point apparatus without calibration. Elemental analyses have been performed by Korea Basic Science Center.

Preparation of $\text{Re}(\equiv\text{NC}_6\text{H}_5)(\text{PPh}_3)(\text{PMe}_3)\text{Cl}_3$, **II.** 0.30 g (0.33 mmol) of **I** and 0.66 ml (0.66 mmol) of PMe_3 (1.0 M in toluene) in 60 ml of benzene were stirred for 36h at room temperature, and then the solvent was removed under vacuum. The resulting green oily product had been stirred in diethyl ether (30 ml) for 2h at room temperature to give green solids. The resulting solids were filtered, washed with benzene (30 ml \times 1) and hexanes (30 ml \times 3), and then dried under vacuum to give 0.10 g (0.13 mmol, 39.4%) of **II**. The product recrystallized from acetone/hexanes. ¹H-NMR (CDCl_3) δ 1.650 (9H, dd, $^2J_{\text{P-H}} = 10.87$ Hz, $^4J_{\text{P-H}} = 1.22$ Hz, PMe_3), 7.007-7.858 (20H, m), ¹³C{¹H} NMR (CDCl_3) δ 12.96 (d, $J_{\text{P-C}} = 138$ Hz, PMe_3), 121.20, 127.79, 127.99, 128.52, 129.59, 130.13, 134.63, 134.81. Anal. Calcd for $\text{C}_{27}\text{H}_{29}\text{NP}_2\text{Cl}_3\text{Re}$: C, 44.91; H, 4.06; N, 1.94. Found: C, 44.62; H, 4.16; N, 1.97. mp. = 178-180 °C. IR (KBr): 3057, 1482, 1435, 1413, 1283, 1093, 1025, 957, 767, 746, 695, 525, 513, 494 cm^{-1} .

Preparation of $\text{Re}(\equiv\text{NC}_6\text{H}_5)(\text{PPh}_3)(\text{P}(\text{OMe})_3)\text{Cl}_3$, **III.** 0.30 g (0.33 mmol) of **I** and 0.79 ml (6.6 mmol) of $\text{P}(\text{OMe})_3$ in 60 ml of benzene were stirred for 36h at room temperature. The resulting solution was concentrated to about 20 ml to precipitate the product as silvery blue solids. The so-

Table 1. Crystallographic Data and Summary of Data Collection and Structure Refinement

	II	III
Formula	C ₂₇ H ₂₉ NP ₂ Cl ₃ Re	C ₂₇ H ₂₉ NO ₃ P ₂ Cl ₃ Re
<i>fw</i>	722.00	770.00
Crystal system	Orthorhombic	Monoclinic
Space group	<i>Pna</i> 2 ₁	<i>P</i> 2 ₁ / <i>n</i>
<i>a</i> , Å	19.379(4)	11.399(3)
<i>b</i> , Å	11.867(2)	14.718(4)
<i>c</i> , Å	12.676(3)	17.558(5)
β, deg		97.79(2)
<i>V</i> , Å ³	2915(1)	2917(1)
<i>d</i> _{calc} g cm ⁻³	1.645	1.752
μ, mm ⁻¹	4.570	4.578
F(000)	1416	1512
<i>Z</i>	4	4
Scan range	3<2θ<50	3<2θ<50
Scan type	ω-2θ	ω-2θ
No. of unique data	2226	3868
No. of reflns	2203	3739
Used, <i>I</i> >2σ(<i>I</i>)		
No. of params	306	344
Max. in Δρ (e Å ³)	0.98	1.00
GOF on <i>F</i> ²	1.041	1.050
<i>R</i>	0.0251	0.0571
<i>wR</i> ₂ ^a	0.0621	0.1384

$$^a wR_2 = \{ \sum [w(F_o^2 - F_c^2)^2] / \sum [w(F_o^2)^2] \}^{1/2}$$

lids were filtered, washed with benzene (30 ml×1), diethyl ether (30 ml×1), and hexanes (30 ml×1), and then dried under vacuum to give 0.09 g (0.12 mmol, 36.4%) of **III**. The product recrystallized from CH₂Cl₂/hexanes. ¹H NMR (CDCl₃) δ 3.690 (9H, d, ³J_{P-H}=10.43 Hz, P(OMe)₃), 7.078-7.893 (20H, m). ¹³C{H} NMR (CDCl₃) δ 55.67 (d, ³J_{P-C}=34 Hz, P(OMe)₃), 125.69, 128.36, 128.57, 129.65, 130.50, 131.15, 131.20, 133.79, 134.83, 135.50, 135.68. Anal. Calcd for C₂₇H₂₉NO₃P₂Cl₃Re: C, 42.11; H, 3.80; N, 1.82. Found: C, 41.77; H, 3.71; N, 1.65. mp.=176-178°C (decom.). IR (KBr): 3063, 2953, 1482, 1436, 1186, 1173, 1092, 1063, 1036, 1010, 810, 795, 770, 746, 692, 564, 525 cm⁻¹.

X-ray Structure Determination. All X-ray data were collected with use of an Enraf-Nonius CAD4 automated diffractometer equipped with a Mo X-ray tube and a graphite crystal monochromator. Details on crystal and intensity data are given in Table 1. The orientation matrix and unit cell parameters were determined from 25 machine-centered reflections with 20<2θ<30°. Axial photographs were used to verify the unit cell choice. Intensities of three check reflections were monitored after every 1h during data collection. Data were corrected for Lorentz and polarization effects. Decay corrections were made. The intensity data were empirically corrected with Ψ-scan data. All calculations were carried out on the personal computer with use of the SHELXS-86⁸ and SHELXL-93⁹ programs.

A green crystal of **II**, shaped as a block, of approximate dimensions 0.3×0.3×0.4 mm, was used for crystal and intensity data collection. The unit cell parameters and systematic

Table 2. Atomic Coordinates (×10⁴) and equivalent Isotropic Thermal Parameters (Å²×10³) for **II**

	<i>x</i>	<i>y</i>	<i>z</i>	<i>U</i> (eq) ^a
Re	9337 (1)	7639 (1)	10000 (0)	27(1)
CL1	9292 (3)	7567 (6)	8109 (6)	38(2)
CL2	9301 (4)	7547 (7)	11926 (8)	55(2)
CL3	8537(8)	6074 (1)	10024 (6)	39(1)
P1	10179 (1)	6131 (2)	9981 (7)	36(1)
P2	8351(9)	9001 (2)	9984 (6)	27(1)
N	9972 (3)	8638 (5)	9956(15)	32(2)
C1	10141(10)	5208(19)	8912(13)	60(7)
C2	11059 (4)	6643 (8)	10183(14)	44(3)
C3	10143(11)	5191(16)	11149(14)	63(7)
C11	8782 (4)	10352 (6)	9988(23)	33(2)
C12	9016 (9)	10912(15)	9044(14)	31(4)
C13	9442(10)	11745(18)	9155(24)	64(8)
C14	9633 (5)	12250 (7)	10037(31)	77(4)
C15	9403(11)	11836(23)	11023(24)	65(7)
C16	8980(11)	10765(18)	10900(18)	59(7)
C21	7758(10)	9113(18)	11139(17)	50(6)
C22	7393(10)	10035(16)	11472(16)	31(4)
C23	6915(11)	9993(24)	12282(22)	51(6)
C24	6793(12)	8985(29)	12788(19)	60(7)
C25	7149(11)	8043(22)	12384(17)	49(5)
C26	7627(11)	8125(20)	11691(18)	53(6)
C31	7761 (6)	8997(13)	8898(12)	18(3)
C32	7578(10)	8014(14)	8408(15)	34(5)
C33	7125 (8)	8073(23)	7455(16)	42(5)
C34	6860(11)	9108(26)	7243(15)	50(6)
C35	7019(11)	10061(23)	7765(23)	49(6)
C36	7486(11)	10036(22)	8611(17)	48(6)
C41	10521 (4)	9388 (7)	9922(23)	32(4)
C42	10780(10)	9789(15)	11071(12)	40(3)
C43	10811(13)	9683(24)	9224(15)	81(8)
C44	11305(13)	10589(21)	11022(22)	68(6)
C45	11644 (6)	10765(11)	10036(24)	100(7)
C46	11405(12)	10307(20)	9157(22)	73(7)

^aEquivalent isotropic *U* defined as one-third of the trace of the orthogonalized *U*_{ij} tensor.

absences, *h*00 (*h*=2*n*+1), 0*k*0 (*k*=2*n*+1), 00*l* (*l*=2*n*+1), 0*k**l* (*k*+*l*=2*n*+1), and *h*0*l* (*h*=2*n*+1), indicated two possible space groups: *Pna*2₁ and *Pnam*. A statistical analysis of intensities suggested a noncentrosymmetric space group, and the structure converged only in the space group *Pna*2₁. The structure was solved by the heavy atom methods. All non-hydrogen atoms were refined anisotropically. All hydrogen atoms were positioned geometrically and refined using a riding model.

A blue crystal of **III**, shaped as a block, of approximate dimensions 0.2×0.3×0.3 mm, was used for crystal and intensity data collection. The unit cell parameters and systematic absences, *h*00 (*h*=2*n*+1), 0*k*0 (*k*=2*n*+1), 00*l* (*l*=2*n*+1), and *h*0*l* (*h*+*l*'=2*n*+1), unambiguously indicated *P*2₁/*n* as a space group. The structure was solved by the heavy atom methods. All non-hydrogen atoms were refined anisotropically. All hy-

Table 3. Atomic Coordinates ($\times 10^4$) and Equivalent Isotropic Thermal Parameters ($\text{\AA}^2 \times 10^3$) for **III**

	<i>x</i>	<i>y</i>	<i>z</i>	<i>U</i> (eq) ^a
Re	-882 (1)	3384 (1)	7109 (1)	29(1)
C11	-1719 (2)	2264 (2)	7887 (2)	43(1)
C12	-563 (3)	2127 (2)	6276 (2)	47(1)
C13	-2837 (3)	3471 (2)	6364 (2)	61(1)
P1	1095 (2)	3045 (2)	7805 (2)	28(1)
P2	-1460 (2)	4243 (2)	8143 (2)	33(1)
O1	-1205 (7)	5285 (5)	8032 (4)	42(2)
O2	-2770 (6)	4202 (6)	8338 (5)	50(2)
O3	-753 (6)	3965 (6)	8942 (4)	44(2)
N	-413 (7)	4327 (6)	6664 (5)	32(2)
C1	-1436(11)	5963 (8)	8591 (7)	48(3)
C2	-3752(11)	4654(11)	7884 (9)	69(4)
C3	-1198(17)	3785(14)	9628(11)	101(6)
C11	2256 (9)	2890 (7)	7188 (6)	33(2)
C12	3385 (9)	2648 (8)	7543 (6)	41(3)
C13	4333 (9)	2606 (9)	7100 (7)	48(3)
C14	4151(10)	2801 (8)	6331 (7)	44(3)
C15	3010(10)	3046 (8)	5977 (7)	39(3)
C16	2069 (8)	3090 (7)	6402 (6)	29(2)
C21	1825 (8)	3899 (7)	8470 (5)	29(2)
C22	2605(11)	3646 (8)	9103 (7)	43(3)
C23	3314(11)	4321 (8)	9533 (7)	49(3)
C24	3197(10)	5198 (9)	9310 (7)	50(3)
C25	2394(10)	5466 (8)	8675 (7)	43(3)
C26	1714 (9)	4811 (7)	8261 (6)	32(2)
C31	1105 (8)	1984 (7)	8348 (6)	30(2)
C32	834(11)	1958 (8)	9095 (6)	42(3)
C33	745(11)	1150 (9)	9454 (7)	52(3)
C34	915(11)	345 (9)	9089 (8)	53(3)
C35	1159(10)	357 (7)	8344 (7)	44(3)
C36	1252(10)	1169 (7)	7982 (7)	36(2)
C41	-272 (9)	5166 (7)	6314 (6)	33(2)
C42	707 (9)	5306 (8)	5927 (7)	40(3)
C43	807(12)	6114 (9)	5546 (7)	53(3)
C44	-48(12)	6781 (8)	5532 (7)	51(3)
C45	-989(12)	6641 (9)	5936 (8)	55(3)
C46	-1120(10)	5835 (8)	6311 (7)	49(3)

^aEquivalent isotropic *U* defined as one-third of the trace of the orthogonalized U_{ij} tensor.

drogen atoms were positioned geometrically and refined using a riding model.

Final atomic positional parameters for non-hydrogen atoms are shown in Table 2 and 3. The selected bond distances and bond angles are shown in Table 4 and 5; anisotropic thermal parameters, hydrogen atom coordinates, full bond distances and bond angles, and tables of observed and calculated structure factors are available as supplementary materials.

Results and Discussions

Preparation of **II** and **III**. *Mer, trans*- $\text{Re}(\text{NPh})\text{Cl}_3(\text{PPh}_3)_2$,

Table 4. Selected Bond Distances (\AA) and Bond Angles (deg) for **II**

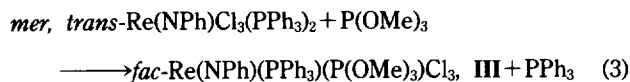
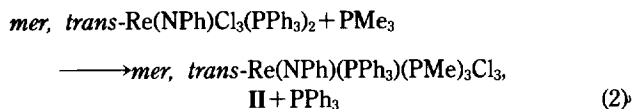
Bond Distances			
RE-CL1	2.400(7)	RE-CL2	2.445(10)
RE-CL3	2.419(2)	RE-P1	2.421 (2)
RE-P2	2.503(2)	RE-N	1.711 (6)
P1-C1	1.74 (2)	P1-C2	1.83 (.8)
P1-C3	1.85 (2)	P2-C11	1.82 (.7)
P2-C21	1.86 (2)	P2-C31	1.79 (1)
N-C41	1.39 (1)		
Bond Angles			
CL2-RE-CL1	174.1(1)	CL3-RE-CL1	87.8(2)
CL3-RE-CL2	86.3(2)	P1-RE-CL1	89.3(3)
P1-RE-CL2	89.8(3)	P1-RE-CL3	82.2(1)
P2-RE-CL1	89.3(2)	P2-RE-CL2	90.9(2)
P2-RE-CL3	90.4(1)	P2-RE-P1	172.5(1)
N-RE-CL1	91.1(7)	N-RE-CL2	94.8(7)
N-RE-CL3	173.7(2)	N-RE-P1	91.5(2)
N-RE-P2	95.8(2)	C11-P2-RE	102.8(2)
C21-P2-RE	120.7(7)	C31-P2-RE	119.5(6)
C41-N-RE	176.0(6)		

Table 5. Selected Bond Distances (\AA) and Bond Angles (deg) for **III**

Bond Distances			
RE-CL1	2.419 (3)	RE-CL2	2.416 (3)
RE-CL3	2.430 (3)	RE-P1	2.465 (3)
RE-P2	2.377 (3)	RE-N	1.710 (8)
P1-C11	1.833(10)	P1-C21	1.836(11)
P1-C31	1.829(10)	P2-O1	1.578 (8)
P2-O2	1.578 (7)	P2-O3	1.575 (8)
O1-C1	1.45 (1)	O2-C2	1.45 (2)
O3-C3	1.40 (2)	N-C41	1.40 (1)
Bond Angles			
CL2-RE-CL1	85.6(1)	CL3-RE-CL1	86.4(1)
CL3-RE-CL2	85.2(1)	P1-RE-CL1	89.2(1)
P1-RE-CL2	86.7(1)	P1-RE-CL3	171.1(1)
P2-RE-CL1	76.1(1)	P2-RE-CL2	161.6(1)
P2-RE-CL3	93.1(1)	P2-RE-P1	93.4(1)
O1-P2-RE	110.4(3)	O2-P2-RE	121.0(3)
O3-P2-RE	112.4(3)	N-RE-CL1	168.7(3)
N-RE-CL2	105.5(3)	N-RE-CL3	91.9(3)
N-RE-P1	93.9(3)	N-RE-P2	92.9(3)
C11-P1-RE	114.7(4)	C21-P1-RE	118.8(3)
C31-P1-RE	111.8(3)	C41-N-RE	167.9(7)

I, reacted with PMe_3 at room temperature to give *mer, trans*- $\text{Re}(\text{NPh})(\text{PPh}_3)(\text{PMe}_3)\text{Cl}_3$, **II**, which recrystallized from acetone/hexanes Eq. (2). **II** is air-stable in a solid form but unstable in solutions. For instance, **II** changed its color from green to brown after 48h in such solvents as dichloromethane and benzene. This situation was also observed for the complex *fac*- $\text{Re}(\text{NPh})(\text{PPh}_3)(\text{CO})\text{Cl}_3$ which was previously prepared by our group.⁶ *Fac*- $\text{Re}(\text{NPh})(\text{PPh}_3)(\text{P}(\text{OMe})_3)\text{Cl}_3$, **III**,

was obtained by a similar reaction, and recrystallized from CH_2Cl_2 /hexanes Eq. (3). **III** was originally prepared by reacting $\text{Re}(\text{O})(\text{PPh}_3)(\text{P}(\text{OMe})_3)\text{Cl}_3$ with aniline.¹⁰ **III** also appeared to be unstable in such solvents as CH_2Cl_2 and THF.



In ^{13}C NMR spectra, both **II** and **III** show a doublet for PMe_3 (δ 12.96, d, $J_{\text{P-C}}=138$ Hz) and $\text{P}(\text{OMe})_3$ (δ 55.67, d, $J_{\text{P-C}}=34$ Hz), due to carbon-phosphorus couplings. In ^1H NMR spectra, methyl protons of PMe_3 in **II** give rise to a sharp doublet of doublets at δ 1.65, indicating that, first, the protons of PMe_3 are strongly coupled to the phosphorus of PMe_3 ($J_{\text{P-H}}=10.87$ Hz), and second, weakly coupled to the phosphorus of PPh_3 *trans* to PMe_3 ($J_{\text{P-H}}=1.22$ Hz). In ^1H NMR spectra, the splitting patterns of phosphine protons of metal bisphosphine complexes in which phosphines are particularly identical alkyl phosphines, are known to be sensitive to the relative orientations of the two phosphines.¹¹ For example, if two phosphine ligands are *cis*, a doublet for the alkyl protons is observed. On the other hand, if they are *trans*, a distorted triplet with a broad central peak is observed, due to the virtual coupling by which alkyl protons appear to be coupled both to its own and to the *trans*-phosphorus nucleus about equally. Although the two phosphines in **II** are *trans*, ^1H NMR spectra of **II** exhibits a doublet of doublets for methyl protons instead of a triplet, probably because of the inequivalent phosphines. ^1H NMR spectra **III** show a sharp doublet at δ 3.69, which indicates a *cis*-orientation of PPh_3 and $\text{P}(\text{OMe})_3$ ligands. The relative orientations of two phosphines in **II** and **III** were concretely confirmed by X-ray diffraction studies, as described later.

The relative orientations of the phosphine ligands in **II** and **III** invoke a fundamental question as to how they were formed. Since the starting material **I** is an 18-electron saturated complex, complex **II** and **III** might be produced from the same 5-coordinate intermediate, which was formed by dissociation of PPh_3 (Scheme 1). In addition, the intermediate appeared to be fluxional, considering the relative orientations of two phosphine ligands in **II** and **III**. In other words, **II** was formed by addition of PMe_3 before the intermediate rearranged and **III** was formed after the intermediate rearranged. These results might be explained in terms of the differences in coordinating abilities between PMe_3 and $\text{P}(\text{OMe})_3$. Trialkylphosphines are known to have more powerful coordinating ability than the corresponding trialkylphosphites.¹² PMe_3 , with the better coordinating ability, appeared to bind to the intermediate to give **II** before the ligand rearrangement, with the retention of configuration around the rhenium metal. On the other hand, $\text{P}(\text{OMe})_3$, with the less coordinating ability compared to PMe_3 , seemed to react somewhat slowly with the fluxional intermediate which has enough time to rearrange. This type of rearrangement of the intermediate **A** (Scheme 1) was also observed in the preparation of *fac*- $\text{Re}(\text{NPh})(\text{PPh}_3)(\text{CO})\text{Cl}_3$ from the reaction of **I** with CO .⁶ At this point we cannot clearly explain how

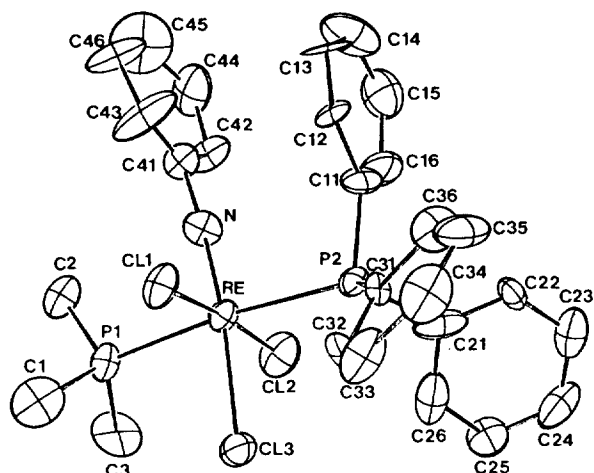
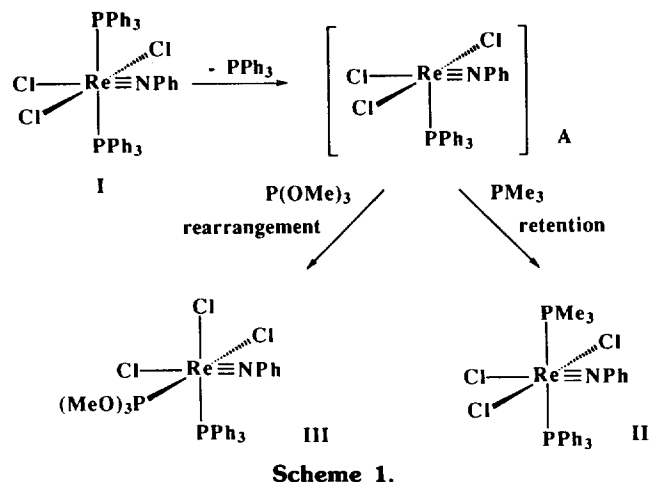


Figure 1. ORTEP drawing of **II** showing the atom-labeling scheme and 50% probability thermal ellipsoids.

the *fac*-orientation of the three Cl ligands in **III** was preferentially formed. However, since the other three ligands in **III**, $\text{P}(\text{OMe})_3$, PPh_3 , and NPh , are relatively strong *trans*-influence ligands, they are expected to prefer *cis*-orientations to each other. These *cis*-orientations maybe play an important role in determining the direction of the ligand rearrangement of the intermediate to produce the *fac*-orientation of the three Cl ligands.

Structure of **II and **III**.** As shown in Figure 1, 2, compound **II** has a NPh group, three *mer*-Cl atoms and *trans*-phosphine ligands, and compound **III** has a NPh group, three *facial*-Cl atoms, and *cis*-phosphine ligands. **II** shows a more distorted octahedral geometry than the starting material **I**¹³ (Table 3). For example, five atoms (Re, N, C11, C12, C13) on the basal plane in **I** and **II** are coplanar within ± 0.01 Å, ± 0.05 Å, respectively, and the bond angles of P-Re-P are $174.1(1)^\circ$ in **I** and $172.5(1)^\circ$ in **II**. The distortion may result from replacing one PPh_3 in **I** by a smaller PMe_3 group.¹² The fact that the dihedral angles between the basal plane (Re, N, C11, C12, C13) and a phenyl ring of phenylimido are $5.2(3)^\circ$ in compound **I** and $12.5(5)^\circ$ in compound **II** also supports the steric repulsion among the phenylimido phenyl ring and two phosphine ligands. In comparison to the

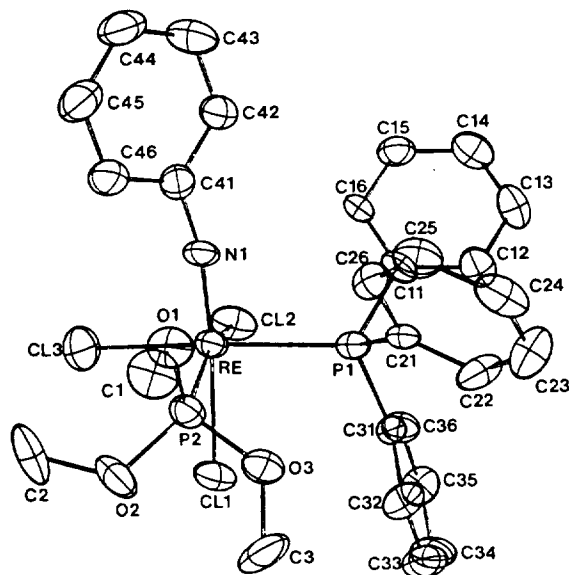


Figure 2. ORTEP drawing of **III** showing the atom-labeling scheme and 50% probability thermal ellipsoids.

starting material **I**, the bond distance of Re-N became shorter from 1.726(6) Å to 1.711(6) Å and the bond angle of Re-N-C(Ph) became essentially linear from 172.6(6)° to 176.0(6)°, indicating that the Re-N bond in **II** is strengthened and has a more triple bond character, and therefore the nitrogen atom has more *s*-character.^{1a}

On the other hand, five atoms (Re, N, C11, C12, P2) on the basal plane in **III** are coplanar within ± 0.02 Å, and the dihedral angle between the basal plane and the phenylimido phenyl ring is 44.8(4)°, which suggests that the steric repulsion among the phenylimido phenyl ring, PPh₃ and P(OMe)₃ is very high. The bond distance (1.710(8) Å) of Re-N in **III** is similar to that (1.711(6) Å) in **II**, but the bond angle of Re-N-C(Ph) (167.9(7)°) in **III** is more distorted from linearity than that (176.0(6)°) in **II**. Structural studies of both **II** and **III** show that the nitrogen atom in both complexes has more *s*-character than that in **I**, and that the *cis*-configuration of PPh₃ and P(OMe)₃ in **III** results in the high steric congestion around the central metal to break more severely the coplanarity between the basal plane and NPh.

The bond distances of Re-Cl (2.419(2) Å in **II**, 2.419(3) Å in **III**), *trans* to N, are longer than that in **I** (2.402(2) Å), suggesting that the imido group has an enhanced *trans*-influence effect in **II** and **III**. The average bond distance of Re-Cl (2.421(6) Å for **II**, 2.423(3) Å for **III**), *trans* to phosphine, in **II** and **III** became longer than that in **I** (2.409(4) Å), in spite of substitution of a smaller PMe₃ (cone angle, $\theta = 118^\circ$), P(OMe)₃ ($\theta = 107^\circ$) for a larger PPh₃ ($\theta = 145^\circ$).¹² These results suggest that an electronic effect of PMe₃ and P(OMe)₃, in addition to their steric effect, on the geometry of **II** and **III** may also be important. The metal-halide bond in a high-valent metal complex frequently has a multiple bond character due to π -bonding from a lone pair of electrons to a vacant *d*-orbital of the metal in the high oxidation state.¹⁴ The elongated bond distances of Re-Cl in **II** and **III** might be explained by the presence of both PR₃ (R = Me in **II**, OMe in **III**) and a more *sp*-hybridized imido group, which

can donate the electron density to the electron-deficient Re metal in the high oxidation state of +5. The Re-P bond distances (2.421(2) Å for Re-PMe₃, 2.465(3)-2.503(2) Å for Re-PPh₃) agree with known values (2.324-2.470 Å, 2.472-2.505 Å, respectively).¹⁵ The Re-P(PPh₃) bond distance of 2.503(2) Å in **II**, *trans* to PMe₃, is longer than that (2.465(3) Å) in **III**, *trans* to Cl, which can be explained on the basis of the known fact that PMe₃ is a stronger *trans*-influence ligand than Cl.¹⁶

In summary, we prepared Re(NPh)(PPh₃)(PR₃)Cl₃ (PR₃ = PMe₃ for **II**, P(OMe)₃ for **III**) from Re(NPh)(PPh₃)₂Cl₃ by replacing one PPh₃ with the corresponding ligands. Structures of these mixed-phosphine complexes have been determined through X-ray diffraction. Structural studies showed that the relative orientations of the two phosphines in both complexes are different, probably due to the differences in the coordinating abilities between PMe₃ and P(OMe)₃ to the 5-coordinate fluxional intermediate.

Acknowledgment. This work is based on research sponsored by the Ministry of Education under grant BSRI-94-3420.

Supplementary Material Available. Tables of bond distances and bond angles, anisotropic thermal parameters, positional parameters for hydrogen atom (8 pages); listings of observed and calculated structure factors (14 pages). Supplementary materials are available from one of the authors (S. W. Lee) upon request.

References

- (a) Nugent, W. A.; Mayer, J. M. *Metal-Ligand Multiple Bonds*; John Wiley and Sons: New York, U. S. A. 1988. (b) Chisholm, M. H.; Rothwell, I. P. In *Comprehensive Coordination Chemistry*; Wilkinson, G.; Gillard, R. D.; J. A. McCleverty, Ed.; Pergamon Press: Oxford, England, 1987; Vol. 2, pp 161-188. (c) Nugent, W. A.; Haymore, B. L. *Coord. Chem. Rev.* **1980**, *31*, 123 (d) Cenini, S.; La Monica, G. *Inorg. Chim. Acta* **1976**, *18*, 279.
- Maata, E. A.; Du, Y.; Rheingold, A. L. *J. Chem. Soc. Commun.* **1990**, 756 and references therein.
- Bakir, M.; Fanwick, P. E.; Walton, R. A. *Inorg. Chem.* **1988**, *26*, 2692 and references therein.
- (a) Gray, S. D.; Smith, D. P.; Bruck, M. A.; Wigley, D. E. *J. Am. Chem. Soc.* **1992**, *114*, 5462. (b) Perot, G. *Catal. Today* **1991**, *10*, 447.
- Glueck, D. S.; Wu, J.; Hollander, F. J.; Bergman, R. G. *J. Am. Chem. Soc.* **1991**, *113*, 2041.
- Kim, Y-W.; Jung, J-H.; Lee, S. W. *Bull. Korean Chem. Soc.* **1994**, *15*, 150.
- (a) Chatt, J.; Diworth, J. R. *J. Chem. Soc. Chem. Commun.* **1972**, 549. (b) Chatt, J.; Garforth, J. D.; Johnson, N. P.; Rowe, G. A. *J. Chem. Soc.* **1964**, 1012.
- Sheldrick, G. M. *Acta Cryst.* **1990**, *A46*, 467.
- Sheldrick, G. M. *SHELXL-93*, University of Gottingen, 1993.
- Johnson, N. R.; Pickfold, Martin, E. L. *J. Chem. Soc., Dalton Trans.* **1976**, 950.
- Crabtree, R. H. *The Organometallic Chemistry of the Transition Metals*; John Wiley and Sons: 2nd ed.; New York, U. S. A. 1994; p 237.
- Tolman, C. A. *Chem. Rev.* **1977**, *77*, 313.

13. Forellini, E.; Casellato, U. *Acta Cryst.* 1984, C40, 1795.
 14. Huheey, J. E.; Keiter, E. A.; Keiter, R. L. *Inorganic Chemistry*; Harper Collins: 4th ed.; New York, 1993; p 420.
 15. Orpen, A. G.; Brammer, L.; Allen, F. H.; Kennard, O.; Watson, D. G.; Taylor, R. J. *Chem. Soc. Dalton Trans.* 1989, S1-S83.
 16. Collman, J. P.; Hegedus, L. S.; Norton, J. R.; Finke, R. G. *Principles and Applications of Organotransition Metal Chemistry*; University Science Book, Mill Valley, 1987; p 67.

pH-Dependent Electrochemical Behavior of N-Monosubstituted-4,4'-Bipyridinium Ions

Joon Woo Park*, Yuna Kim, and Chongmok Lee

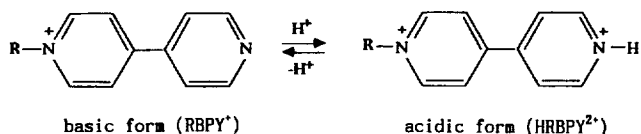
Department of Chemistry, Ewha Womans University, Seoul 120-750, Korea

Received July 19, 1994

The pH-dependent reduction behavior of N-monosubstituted-4,4'-bipyridinium ions (RBPY⁺; R=methyl(C₁); benzyl; n-octyl; n-dodecyl) has been investigated by electrochemical and spectroelectrochemical techniques. At acidic condition, RBPY⁺ is protonated and the protonated species are reduced by two consecutive one-electron processes. The 2e⁻ reduced species undergoes a chemical reaction with H⁺. The second-order rate constant (*k_H*) of the homogeneous chemical process is (3.7 ± 0.3) × 10³ M⁻¹s⁻¹ for the two electron reduction product of C₁BPY⁺. At high pH, the electrode reduction of RBPY⁺ is one-step 2e⁻ transfer process with concomitant addition of H⁺, which is confirmed by cyclic voltammetric study using a microdisk electrode.

Introduction

N-monosubstituted-4,4'-bipyridinium ions (RBPY⁺) are closely related with N,N'-disubstituted-4,4'-bipyridinium ions (viologens) via the following acid-base equilibrium.



The acidic form has structural similarity to viologens which are very attractive materials as electron-transfer reagent in chemical¹ and photochemical² reductions of substrates, solar energy conversion,³ and electrochromic display.⁴ The basic form is a substituted pyridinium and can be considered as a coenzyme NAD⁺ analogue. Because of these interesting characters, the pH-dependent electrochemical^{5,6} and spectroscopic^{7,8} behaviors of the RBPY⁺ compounds as well as their ability as electron carriers⁹⁻¹¹ in redox reactions have been investigated. Recently, Ishida *et al.*¹¹ reported that the interaction between CO₂ and electrochemically reduced species of N-propyl-4,4'-bipyridinium cation (C₃BPY⁺) activates the electron transfer from the bipyridine ring to CO₂. They also claimed that C₃BPY⁺ is reduced by 1e⁻ process at -1.0 V (*vs* SCE) in acetonitrile media. We have been interested in electrochemical behavior of viologens^{12,13} and the reactions of the reduced NAD⁺, NADH, and their analogues.^{14,15} In this paper, we present the pH-dependent reduction behavior of RBPY utilizing electrochemical and spectroelectrochemical techniques. Cyclic voltammetry (CV) with a microdisk electrode is used to determine the number of elec-

trons transferred in the reduction reactions. Also, the reaction rate of the electrogenerated 2e⁻ reduction product of C₁BPY⁺ in acidic medium is determined.

Experimental

Materials. N-monosubstituted-4,4'-bipyridinium (RBPY⁺; R=methyl (C₁); benzyl (B); n-octyl (C₈); n-dodecyl (C₁₂)) salts were prepared by reacting 4,4'-bipyridine with corresponding alkyl or benzyl halides according to known procedure.⁹ Solutions of desired pH were prepared by appropriate mixing of 0.10 M HCl, 0.01 M NaOH+0.09 M NaCl, or 0.01 M Na₂HPO₄+0.07 M NaCl solutions. Reverse osmosed water which was further purified by passage through a purification train (Millipore Corp) was used.

Apparatus and procedures. Cyclic voltammetry (CV) was carried out with a BAS 100B electrochemical analyzer or a Tacussel PRG 5 potentiostat coupled with a GSTP3 function generator. Glassy carbon electrodes (Metrohm and BAS, area of 0.06-0.07 cm²) were polished using 0.1 μm alumina followed by sonication in pure water. A carbon microdisk electrode having a nominal diameter of 11 μm was prepared¹⁶ and used. All potentials are reported against a saturated calomel electrode (SCE) unless otherwise specified. Solutions were purged with nitrogen to remove oxygen. Current was calculated by subtracting the background CV data taken without RBPY⁺ from CV data recorded with RBPY⁺. A Hewlett-Packard 8452A diode array spectrophotometer was used to obtain absorption spectra where the potential of the working electrode (ITO coated glass, Delta Technologies) was controlled potentiostatically.